CELLULAR REPROGRAMMING
Volume 15, Number 5, 2013

DOI: 10.1089/cell.2012.0081

Tracking Induced Pluripotent Stem Cells–Derived Neural Stem Cells in the Central Nervous System of Rats and Monkeys

Hailiang Tang,[1,5] Hongying Sha,[2,5] Huaping Sun,[3,5] Xing Wu,[1] Liqian Xie,[1] Pu Wang,[1] Chengshi Xu,[1] Christian Larsen,[1] Helen L. Zhang,[1] Ye Gong,[1] Ying Mao,[1] Xiancheng Chen,[1] Liangfu Zhou,[1] Xiaoyuan Feng,[3] and Jianhong Zhu[1,4]

Abstract

Despite of the immense breakthroughs of induced pluripotent stem cells (iPSCs), clinical application of iPSCs and their derivates remains hampered by a lack of definitive *in vivo* studies. Here, we attempted to track iPSCs-derived neural stem cells (NSCs) in the rodent and primate central nervous system (CNS) and explore their therapeutic viability for stem cell replacement in traumatic brain injury (TBI) rats and monkeys with spinal cord injury (SCI). Superparamagnetic iron oxide (SPIO) particles were used to label iPSCs-derived NSCs *in vitro*. Labeled NSCs were implanted into TBI rats and SCI monkeys 1 week after injury, and then imaged using gradient reflection echo (GRE) sequence by 3.0T magnetic resonance imaging (MRI) scanner. MRI analysis was performed at 1, 7, 14, 21, and 30 days, respectively, following cell transplantation. Pronounced hypointense signals were initially detected at the cell injection sites in rats and monkeys and were later found to extend progressively to the lesion regions, demonstrating that iPSCs-derived NSCs could migrate to the lesion area from the primary sites. The therapeutic efficacy of iPSCs-derived NSCs was examined concomitantly through functional recovery tests of the animals. In this study, we tracked iPSCs-derived NSCs migration in the CNS of TBI rats and SCI monkeys *in vivo* for the first time. Functional recovery tests showed obvious motor function improvement in transplanted animals. These data provide the necessary foundation for future clinical application of iPSCs for CNS injury.

Introduction

The fact that the entire central nervous system (CNS) is generated from neural stem cells (NSCs) provides the rationale for using NSCs to recapitulate CNS development in restoring the damaged CNS (Breunig et al., 2011). Furthermore, the NSCs derived from induced pluripotent stem cells (iPSCs) offer more promising hope for personalized regenerative disease including CNS injury (Robinton and Daley, 2012). However, before iPSCs and their derivates can be applied in a clinical context, it is critical to evaluate their *in vivo* fate following preclinical transplantation in host animals, especially primates that are physiologically more similar to humans. For example, will the transplanted cells be able to survive in the CNS? Can the transplanted cells find their ways to the lesion? And how can we track their migration to the injury using noninvasive methods to test their safety and effectiveness?

Previously, we reported the first clinical study about tracking migration of NSCs labeled with superparamagnetic iron oxides (SPIO) by magnetic resonance imaging (MRI) for brain trauma patients (Zhu et al., 2006). To address the problems above and assess the viability of iPSCs transplants for CNS injury, we tried to track the distribution of iPSCs-derived NSCs noninvasively in traumatic brain injury (TBI) rats and spinal cord injury (SCI) monkeys *in vivo* in this

[1]Department of Neurosurgery, Huashan Hospital, Fudan University, Shanghai, 200040, China.
[2]National Key Laboratory for Medical Neurobiology, Shanghai Medical College, Fudan University, Shanghai, 200032, China.
[3]Department of Radiology, Huashan Hospital, Fudan University, Shanghai, 200040, China.
[4]National Key Laboratory for Medical Neurobiology, Institute of Brain Science, Shanghai Medical College, Fudan University, Shanghai, 200032, China.
[5]These authors contributed equally to this work.

study. Moreover, functional experiments showed great improvement of motor function in the animals.

Materials and Methods

Derivation of human iPSCs

Human fibroblasts (HFs) were isolated according to the classical method (Villegas and McPhaul, 2005) from the scalp tissue of patients with open brain trauma during emergency surgery after consent. iPSCs induction was based on the method described by the Yamanaka group (Takahashi et al., 2007a; Takahashi et al., 2007b). Briefly, HFs were seeded at 5×10^5 cells per 100-mm dish covered by feeder cells. On the next day, HFs were incubated in a cocktail of retroviruses carrying Oct4, Sox2, Myc, and Klf4 for 24 h. Three days after infection, infection medium was changed with human embryonic stem cells (ESCs) medium. iPSCs selection was performed according to the morphology of human ESC colonies. The characterization of iPSCs includes pluripotent markers expression and *in vivo* and *in vitro* differentiation into the three embryonic germ layer lineages. The detailed methods were performed as previously described (Takahashi and Yamanaka, 2006). The primers for RT-PCR in this study were listed in Table 1.

Induction of human iPSCs into NSCs

Induction of iPSCs was performed by the protocol developed by Chambers et al. (2009) with slight modifications. Briefly, iPSCs cultures were disaggregated using TrypLE™ Express (Invitrogen, Carlsbad, CA, USA) for 5 min, washed using human ESC medium, and preplated on gelatin for 1 h at 37° in the presence of ROCK inhibitor to remove mouse embryonic fibroblasts (MEFs). The nonadherent iPSCs were washed and plated on Matrigel at a density of 18,000 cells/cm^2 in human ESC medium with 10 ng/mL of fibroblast growth factor-2 (FGF-2) and ROCK inhibitor. After iPSCs were nearly confluent, the ROCK inhibitor was withdrawn. The initial differentiation media conditions included knockout serum replacement medium with 10 mM SB431542 (Tocris) and 500 ng/mL of Noggin (R&D). Upon day 5 of differentiation, SB431542 was withdrawn and increasing amounts of N2 medium (25%, 50%, 75%) were added to the knockout serum replacement medium every 2 days while maintaining 500 ng/mL of Noggin. After day 11 of differentiation, the cells were digested and plated in NSCs medium for sphere culture. After culturing for more than 10 generations, the cells were used for immunocytochemistry analysis and labeling experiments.

Electrophysiology evaluation

For electrophysiological recordings, functional analysis of new neurons (differentiated by NSCs) was carried out in the voltage-clamp and current-clamp modes at room temperature. The internal solution for voltage-clamp recordings contained (in mM): 140 CsCl, 10 NaCl, 0.1 $CaCl_2$, 2 $MgCl_2$, 10 HEPES, 1 EGTA (pH 7.2, 310 mOsm). The internal solution for current-clamp recordings contained (in mM): 140 KCl, 0.5 EGTA, 5 HEPES, and 3 Mg-ATP (pH 7.3, 300 mOsm). The external bath solution contained (in mM): 142 NaCl, 3 KCl, 1 $CaCl_2$, 1 $MgCl_2$, 10 D-glucose, and 10 HEPES (pH 7.3, 320 mOsm). Whole-cell recordings were made in current-clamp mode with a Multiclamp 700B amplifier (Axon instruments). Electrodes had resistances of 2–4 MΩ when filled with intracellular solution (in mM): 150 K-gluconate, 10 HEPES, 0.2 EGTA, 4 KCl, 2 NaCl, 14 phosphocreatine, 2 Mg-ATP, and 0.3 Na-GTP (pH 7.35, 305 mOsm). Data were filtered at 10 kHz, digitized at 20 kHz, and analyzed with Clampfit 9.2 (Axon instruments).

Preparation of SPIO-labeled NSCs

NSCs were digested into single cells with Tryple™ Express. Then single cells were labeled with Feridex and green fluorescent protein (GFP) (Zhu et al., 2006). After incubation with SPIOs overnight, the Prussian Blue (PB) method was used for the detection of iron within cell plasma. Two days after SPIO labeling, cells were replated in SPIO-free growth medium. About 7 days later, neurospheres formed by SPIO-labeled cells were processed for labeling efficiency, cell proliferation, and differentiation, as well as electron microscopy analysis (Neri et al., 2008).

TBI rats and SCI monkeys models

The surgical procedures of TBI rats were performed according to the literature already described in detail (Feeney et al., 1981). All animal studies were approved by the Institutional Animal Care and Use Committee of Fudan University (20110307-020). 30 male adult healthy Sprague-Dawley (SD) rats were anesthetized with 10% chloral hydrate (0.32 mL/100g) administered intraperitoneally (i.p.). A controlled cortical impact device was used to induce the injury (Dixon et al., 1991; Postmantur et al., 1997). Rats were placed in a stereotactic frame, and two craniotomies were performed adjacent to the central suture, midway between lambda and bregma. The dura was kept intact over the cortex. Injury was induced by impacting the right cortex with a 3-mm-diameter tip at a rate of 5 cm/sec and a 2-mm compression. Velocity was measured by the linear velocity

Table 1. Primers for Quantitative and Semiquantitative PCR Analysis

Gene name	*Forward primer (5′ to 3′)*	*Reverse primer (5′ to 3′)*
tgOct4	CCCCAGGGCCCCATTTTGGTACC	TTATCGTCGACCACTGTGCTGCTG
tgSox2	GGC ACC CCT GGC ATG GCT CTT GGC TC	
tgKlf4	ACG ATC GTG GCC CCG GAA AAG GAC C	
Oct4	CTGGGTTGATCCTCGGACCT	CACAGAACTCATACGGCGGG
Sox2	CCCAGCAGACTTCACATGT	CCTCCCATTTCCCTCGTTTT
Nanog	AAAGAATCTTCACCTATGCC	GAAGGAAGAGGAGAGACAGT
Gapdh	GTGGACCTGACCTGCCGTCT	GGAGGAGTGGGTGTCGCTGT

displacement transducer. The second craniotomy was for cell injection.

Rhesus monkey SCI models were generated according to the Allen method (Allen and Mac Phail, 1991). All animal studies were approved by the Institutional Animal Care and Use Committee of Fudan University (20110307-020). A laminectomy was performed to expose the spinal cord at the T9 level in six rhesus monkeys provided by animal research center of Fudan University, Shanghai, China. A contusive injury was introduced to each monkey using a 50-gram weight dropped from a height of 10 cm onto a 10-mm^2 impact plate through a guide tube. Traumatized rhesus monkeys were randomly divided into three groups, with two monkeys each.

iPSCs-derived NSCs transplantation in TBI rats and SCI monkeys

One week after TBI, the 30 rats were anesthetized again, and divided randomly into three groups, each with 10 rats. Group 1 rats received 10 μL of human NSCs labeled with SPIO (about 1×10^5 cells) bolus injection at a site about 3 mm from the edge of the lesion. Group 2 rats received 10 μL of phosphate-buffered saline (PBS) treatment. Group 3 rats did not receive cell implantation or PBS injection.

At 1 week after injury, monkeys in group 1 received 10 μL of human NSCs labeled with SPIO (about 1×10^5 cells) bolus injection around the edge of the lesion at T10 level. Monkeys in group 2 received 10 μL of PBS injection at the same level. The remaining two monkeys in group 3 did not receive cell or PBS implantation.

All rats and monkeys of group 1 were administrated immunosuppressant cyclosporine A (i.p. injection, 10 mg/kg) therapy daily and nursing care following NSCs implantation.

In vivo *MRI scanning*

MRI for rats and monkeys was performed with clinical 3.0T systems (Signa, General Electric). For rats, MRI analysis was performed at 0, 1, 14, and 30 days following NSCs transplantation, respectively. For monkeys, MRI analysis was performed at 1, 14, 21, and 30 days following NSCs transplantation, respectively. Gradient reflection echo (GRE) sequence scanning was performed using the following image parameters: echo time (TE) = 6.8 msec; repetition time (TR) = 120 msec; flip angle = 30°; field of view (FOV) = 6; slice thickness = 1.2; number of excitations (NEX) = 4.

PB staining of rat brain sections and immunohistochemistry analysis

All rats were sacrificed and perfused transcardially with 4% polyformaldehyde (PFA) after the last time point of MRI analysis. Brain tissues were fixed in 4% PFA overnight, dehyrated in 30% sucrose solution, frozen on dry ice, and cryosected as 30-μm slices for histology according to the MRI images. The sections were doubly stained by Hematoxylin & Eosin (H&E) and PB to detect intracellular iron oxide particles (Shapiro et al., 2006).

Immunohistochemistry was performed to detect the transplanted NSCs and their derivates features. Brain slices were washed three times with PBS, and the slices were permeabilized for 30 min with 0.25% Triton X-100. Then the brain slices were blocked for 1 h and incubated overnight at 4°C with Nestin, β-tubulin, and glial fibrillary acidic protein (GFAP; Millipore CBL412, AB1540, 1:100), diluted with blocking solution. The slices were washed three times with PBS. Secondary antibodies used were Fluor 555 donkey anti-mouse and 555 donkey anti-rabbit (Invitrogen, 1:500). Nuclei were stained with 1 mg/mL Hoechst 33342 (Invitrogen), and images were observed using a fluorescent microscope.

Functional recovery of injured animals

The behavior of TBI rats grafted with NSCs derived from iPSCs was evaluated by using a neurological severity score and rotarod motor test. The neurological severity score is a composite of the motor, sensory, and reflex tests. One point was given for each failure to perform a task, with a maximum of 14 points. The neurological severity scores were measured for all rats on days 1, 7, 14, 21, and 30 after cell administration. For the rotarod motor test, rats were placed on an accelerating rotarod treadmill and tasked to walk and maintain balance on a rotating rod that gradually increases rotation. The endurance time was recorded in seconds when rats fall off the rod. The rats were tested on days 1, 7, 14, 21, and 30 after cell administration. All measurements were performed by observers who were blinded to individual treatment. Movement assessment of monkeys was performed independently by two investigators blinded to the experiment using the modified Tarlov criteria (Henrich et al., 1996).

Statistical analysis

The Student *t*-test was used to test the difference of proliferation and differentiation between SPIO-labeled and unlabeled NSCs, and the measurement of neurological severity score and rotarod motor test. Probabilities (p value) < 0.05 were regarded as statistical significance.

Results

Pluripotency of human iPSCs and iPSCs-derived NSCs

We first isolated HFs from the scalp tissue of patients with open brain trauma during emergency surgery after consent. Then iPSCs were successfully reprogrammed from HFs by the Yamanaka method (Takahashi et al., 2007b). The characteristics of the iPSCs were similar to human ESCs in morphology (Fig. 1A), and these iPSCs were positive for alkaline phosphatase (AP). The biological potency and epigenetic state of human iPSCs were also determined to be indistinguishable from those of human ESCs. Human iPSCs expressed human ESC-specific surface antigens, including SSEA-4, SOX2, and OCT4 proteins (Fig. 1B–D). Chromosomal G-band analyses showed that human iPSCs had a normal karyotype (Fig. 1E).

Differentiation assays *in vivo* and *in vitro* showed human iPSCs could differentiate into cells of all three germ layers. Human iPSCs were transplanted subcutaneously into a severe combined immunodeficiency (SCID) mouse and a tumor developed from the injection site. Teratomas derived from human iPSCs included neural tissue (ectoderm), muscle tissue (mesoderm), and glandular tissue (endoderm) (Fig. 1F–H). The differentiated iPSCs were positive for cells of all three germ layers, including the endodermal (SOX17), mesodermal (ACTIN), and ectodermal (TUBLIN) lineages.

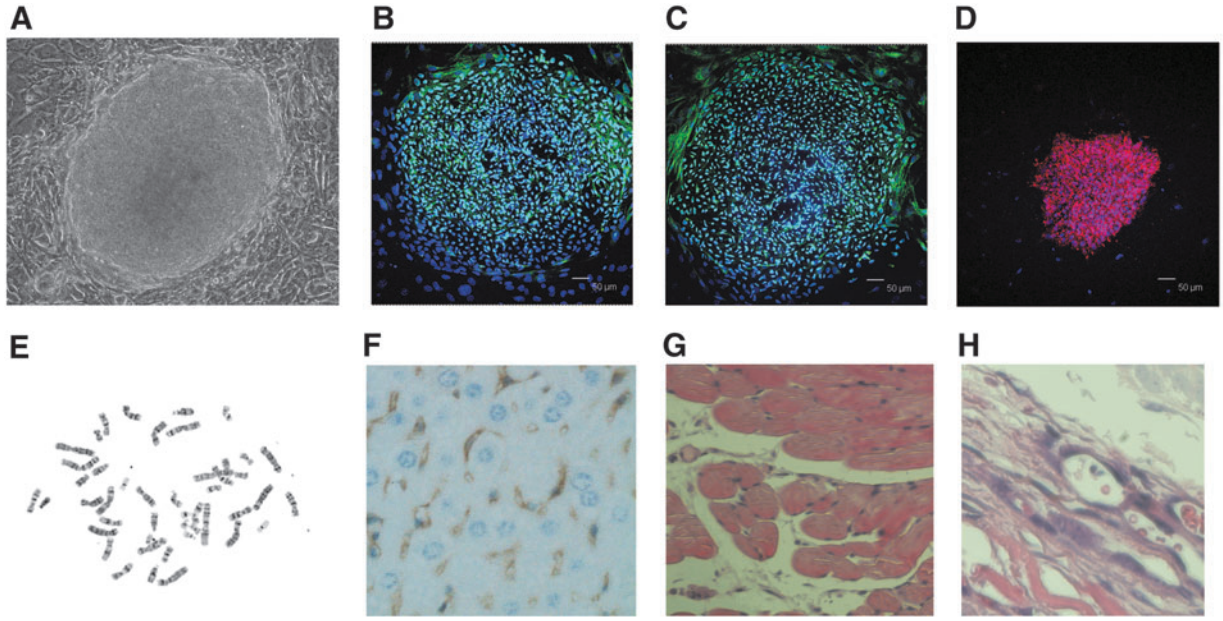

FIG. 1. Human iPSCs and pluripotency. Human iPSCs reprogrammed from HFs exhibited similar characters to human ESCs. (**A**) Morphological properties of human iPSCs present classical features of human ESCs. (**B–D**) Human iPSCs were positive for Oct4, Sox2, and SSEA-4. (**E**) Chromosomal G-band analyses showed that human iPSCs had a normal karyotype. (**F–H**) Teratoma derived from human iPSCs included neural tissue (ectoderm), muscle tissue (mesoderm), and gut like epithelial tissues (endoderm). Scale bar, 50 μm.

RT-PCR analysis showed that ESC marker genes *Oct3/4*, *Nanog*, and *Sox2* were expressed in human iPSCs at levels equivalent to those in human ESCs. Western blot analysis showed that expression of ESC marker genes *Oct3/4*, *Nanog*, and *Sox2* in human iPSCs was also similar to human ESCs. Exogenous gene-specific quantitative PCR analysis demonstrated that the viral transgenes were silenced, because the transgene expression in the iPSCs was very low compared with the infected fibroblast.

To efficiently induce the iPSCs into NSCs, the protocol of Chambers et al. (2009) was applied with some modifications. Briefly, the adherent iPSCs were induced by a dual inhibition of SMAD signaling using Noggin and SB431542. When Noggin and SB431542 were present for 24 h, rosette structure was observed. After 11 days, these cells were digested into single cells and replated in NSCs medium for suspension culture. At 24 h after plating, the aggregates of dividing cells formed spheres (Fig. 2A). Then the cells were cultured for more than 10 generations under suspension status. Immunocytochemistry analysis showed cells in spheres were almost nestin positive (Fig. 2B). In Dulbecco's modified Eagle medium (DMEM) + 10% fetal calf serum (FCS) for an additional 3–6 days, these cells could differentiate into GFAP or tubulin-positive cells (Fig. 2C). The new neurons differentiated by NSCs could generate action potential *in vitro* by electrophysiological recordings (Fig. 2D).

SPIOs-labeled NSCs

To detect iPSCs-derived NSCs by molecular imaging method, the NSCs were labeled with Feridex *in vitro* for 24 h. We found 90% of cells were labeled with SPIOs determined by PB staining (Fig. 2E). Electron microscopy showed dark electron-dense cytoplasmic granular inclusions in cells (Fig. 2F). No significant difference was observed in cell survival, self-renewal, and proliferation capacity between SPIO-labeled and unlabeled NSCs, indicating that the levels of intracellular iron accumulation did not induce acute cell toxicity (Fig. 2G). We also compared the differentiation potential of SPIO-labeled and unlabeled NSCs *in vitro*. After 7–10 days under differentiation conditions, an average of 35%, 55%, and 20% of SPIO-labeled NSCs were nestin positive, β-tubulin positive, and GFAP positive. No significantly statistical difference was observed between the two groups (Fig. 2H).

Targeted migration of SPIO-labeled NSCs in TBI rat brains

In group 1 of TBI rats, we detected some marked signal change on a T2-weighted MRI over time. Pronounced hypointense signals were not found at the injection sites before NSCs implantation (Fig. 3A, 0 days, black arrow). However, the hypointense signals in the injection sites were visible as areas of dark tissue following NSCs implantation (Fig. 3A, 1 day, white arrow). About 2 weeks after cell implantation, the hypointense signals at the injection site faded a little and directed to the lesion region (Fig. 3A, 14 days, red arrow). About 4 weeks after cell administration, the signals around the lesion intensified (Fig. 3A, 30 days, red arrow). The observation from 1 day to 1 month after cell implantation suggested that the iPSCs-derived NSCs could not only survive but could also migrate from the primary injection sites to the border of the damaged area in TBI rats. PB staining of brain sections of group 1 rats showed there were SPIO-labeled cells within the lesion (Fig. 3B), indicating the geographical integration of the transplanted cells with host structures. On the contrary, in group 2 and 3 TBI rats, we did

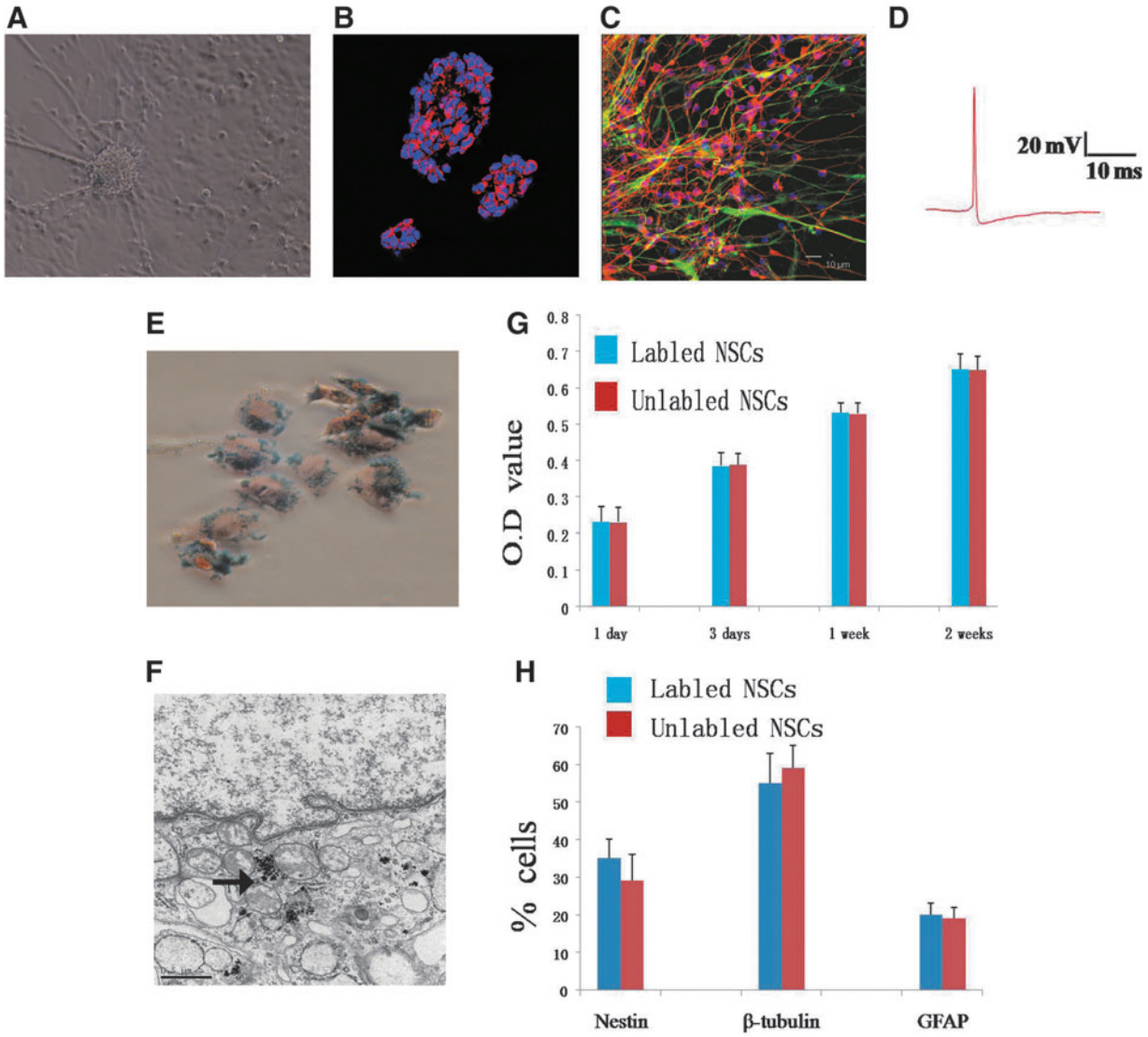

FIG. 2. NSCs derived from human iPSCs. (**A**) Human iPSCs were efficiently induced into neural spheres and mature neural cells in defined culture system. (**B**) iPSCs-derived neural spheres expressed Nestin. (**C**) iPSCs-derived neural cells were positive for GFAP or tubulin. (**D**) New neurons differentiated by NSCs could generate action potentials *in vitro* by electrophysiological recordings. (**E**) Human iPSCs-derived NSCs treated with SPIOs showed intracellular iron accumulation, as visualized by PB staining (blue particles). (**F**) Electron micrographs of SPIO-labeled NSCs revealed the presence of iron nanoparticles (the black arrow) in the cytoplasm at 1 week after culture. (**G**) Proliferation of SPIO-labeled (blue bars) and unlabeled NSCs (red bars) exhibited no significantly statistic difference. Values are mean ± standard deviation, $p > 0.05$. (**H**) Differentiation of SPIO-labeled (blue bars) and unlabeled (red bars) NSCs present no difference. Values are means ± standard deviation, $p > 0.05$. Scale bar, 50 μm.

not observe any pronounced signal changes around the injection sites or the lesion (Fig. 3C, MRI scan of group 2 rat).

To further observe the functional recovery, we examined the behavior of TBI rats grafted with human iPSCs-derived NSCs via the measurement of neurological severity score and rotarod motor test (Mahmood et al., 2001). From 14 to 30 days after NSCs injection, the neurological severity scores of group 1 rats significantly declined, as compared with the group 2 and group 3 rats ($p < 0.01$) (Fig. 3D). During the period, the percentage of duration on the rotarod test also showed significant improvement in group 1, as compared with groups 2 and 3 ($p < 0.01$) (Fig. 3E). The data indicated that the transplanted NSCs could reduce motor and neurological deficits in TBI rats.

H&E staining of brain sections of group 1 rats showed there were no abnormal cells within the brain lesion area, indicating that the transplanted NSCs could not form teratoma (Fig. 3F). The immunohistochemistry of rat brain sections were also performed to detect the implanted NSCs and its offspring in the lesion. The GFP-positive cells were first found in the slides under microscopy (Fig. 3G). These cells were specifically derived from the implanted human NSCs. Results of the immunohistochemistry showed that β-tubulin–positive cells were found in the lesion sites (Fig. 3H), which were not detected in the control slides (Fig. 3I). These data showed that the implanted NSCs could not only migrate to the lesion site, but could also differentiate into functional neural cells and participate in the local neural circuit.

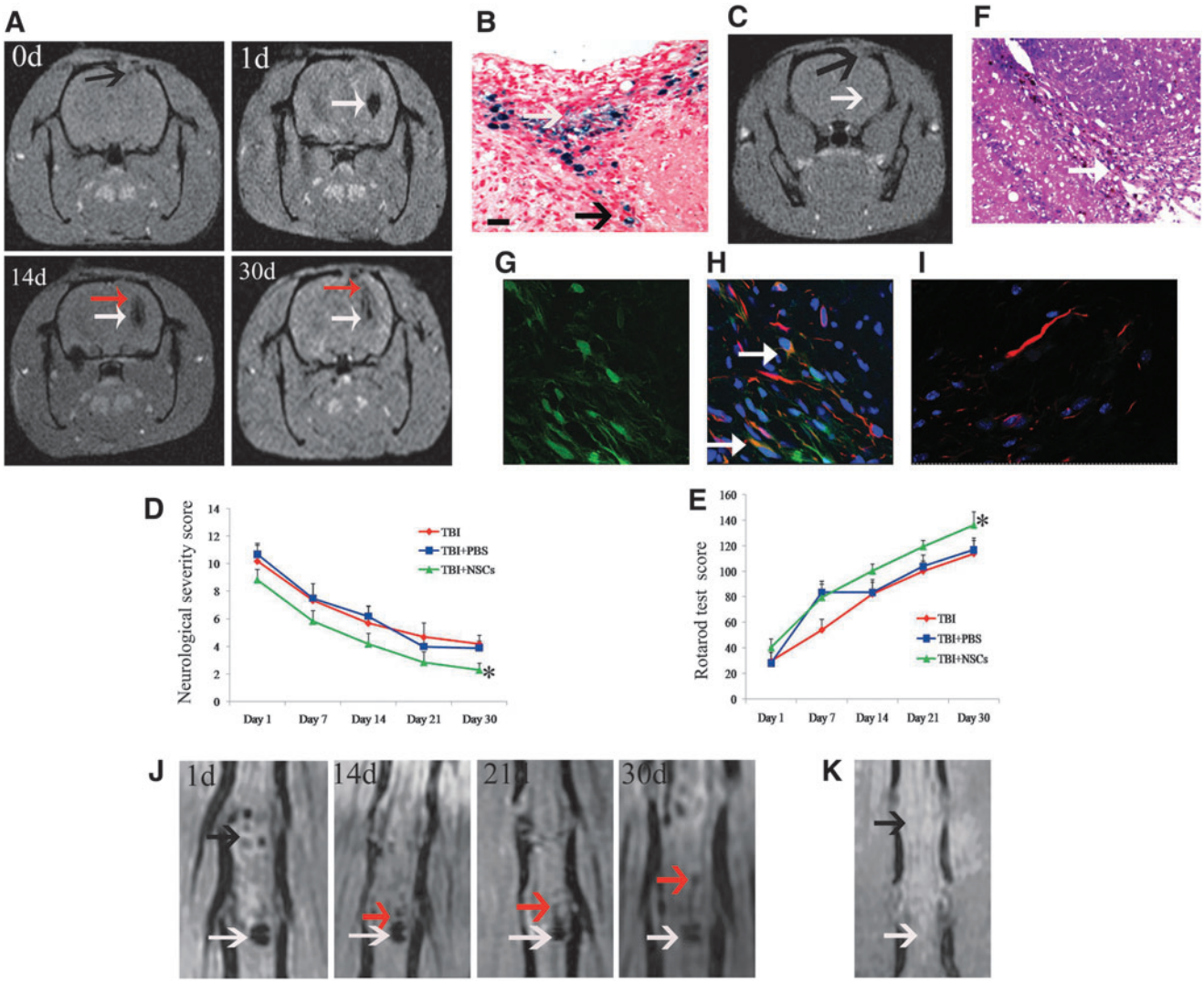

FIG. 3. SPIO-labeled iPSCs-derived NSCs could survive and migrate to the lesion after transplantation in animal model. (**A**) MRI scans of TBI rats that received NSCs transplantation were performed on days 0, 1, 14, and 30 after cell implantation. 0d, MRI scan obtained before SPIO-labeled NSCs implantation showed the lesion (black arrow indicates lesion); 1d, hypointense signals were observed at NSCs injection site on day 1; 14d, dark signals spread from the injection site to the border of the damaged brain region (white arrow indicates cell injection site, red arrow indicates migrated cells); 30d, the dark signal extended further into the lesion (white arrow indicates cell injection site, red arrow indicates migrated NSCs). (**B**) PB staining of rat brain section showed SPIO-labeled NSCs around the cerebral contusion (upper white arrow); the lower black arrow indicates the "migration line" toward the lesion area. (**C**) MRI scan of group-2 rat (PBS group); black arrow shows the lesion, white arrow shows the PBS injection site. (**D**) Neurological severity score at different times after TBI in rats. (**E**) Rotarod test scores at different times after TBI in rats. Values are mean ± standard deviation. (*) $p < 0.01$, compared with TBI and TBI + PBS groups at days 14, 21, and 30 after TBI ($n = 10$). (**F**) H&E staining of brain sections of group-1 rats showed there was no tumor formation within the brain lesion area. Magnification, 100×. (**G**) The GFP-positive human cells were found on the slides of sections within the brain lesion area. (**H**) The immunohistochemistry of rat brain sections showed β-tubulin–positive cells were detected in the lesion area (indicated by white arrows). (**I**) Brain section immunohistochemistry of the control group rats did not show β-tubulin/GFP-positive human cells. (**J**) MRI scans of monkeys with spinal cord injuries that received SPIO-labeled NSCs treatment were performed on days 1, 14, 21, and 30 after cell transplantation. 1d, hypointense signals were observed at cell injection site on day 1 (black arrow indicates lesion region, white arrow indicates cell injection site); 14d and 21d, the hypointense signals spread from the injection site to the border of the damaged region (red arrow indicated cell migration); 30d, NSCs migration stream (red arrow) was clearly detected by MRI. (**K**) In the MRI scan of group-2 monkeys (PBS group), the black arrow shows the lesion and the white arrow shows PBS injection site. Scale bar, 100 μm.

Migration of SPIO-labeled NSCs in monkeys

For SCI monkeys of group 1, similar to the results in group 1 rats, the MRI scan showed cell injection sites as circular areas of dark tissue on day 1 after SPIO-labeled NSCs implantation (Fig. 3J, 1 day, lesion indicated by black arrow, injected site indicated by white arrow). About 2 weeks after cell implantation, the hypointense signals faded a little around the injection site and extended to the lesion region (Fig. 3J, 14 days, red arrow). The hypointense signals around

the lesion area intensified 1 month after NSCs injection, and cell migration was clearly detected on MRI as a hypointense signal "stream" extending from the cell injection site toward the injured region (Fig. 3J, 21 days and 30 days, red arrow), indicating that the iPSCs-derived NSCs could survive and migrate from the cell injection site to the border of the lesion area in SCI monkeys.

Meanwhile, the recovery of neurologic motor function in those monkeys was graded by the modified Tarlov criteria (Henrich et al., 1996). The monkey in group 1 showed paralysis and no movement of both lower limbs on day 1 after cell transplantation (video, day 1 after cell transplantation; Supplementary Data are available at www.liebertpub.com/cell). Day 14 after cell transplantation, the monkey was able to bend its right knee, but showed no capability of climbing and crawling (video, day 14 after cell transplantation). Day 30 after cell transplantation, the monkey was almost fully recovered and showed ability of crawling and climbing (video, day 30 after cell transplantation). Whereas no pronounced signal change around the injection site or the lesion was observed (Fig. 3K shows an MRI scan of a group 2 monkey), and significant recovery signs were either absent in the control groups (data not shown).

Discussion

In the current study, we have shown that adult human fibroblasts reprogrammed by retroviral transduction of the four transcription factors Oct4, Sox2, Klf4, and c-Myc can be converted to iPSCs and differentiate into functional NSCs *in vitro*. We also demonstrated that when injected into TBI rat brains and SCI monkeys, iPSCs-derived NSCs labeled with SPIO particles could be tracked using MRI *in vivo*. Our data illustrated that transplanted NSCs migrated to damaged regions of the brain and injured spinal cord, as denoted by movement of hypointense signals on MRI images. The implantation of NSCs, along with the relative functional recovery of animals that received cell transplants, provides evidence for the therapeutic value of directly reprogrammed fibroblasts for cell replacement therapies in the adult brain and spinal cord.

Studies showed reprogramming of human somatic cells can be achieved by ectopic expression of transcription factors. However, the reprogramming process is inefficient, which is related to the epigenetic status of the reprogrammed cell DNA (Jaenisch and Young, 2008). In our study, we successfully obtained iPSCs from HFs. The characteristics of the iPSCs were similar to human ESCs in morphology and pluripotency (Fig. 1). These iPSCs were then induced into NSCs with typical morphology and differentiation ability (Fig. 2).

With rapid developments in cell biology, particularly in the area of stem cell research, interest in the therapeutic potential of stem cells has increased. To detect the dynamics of stem cell migration and differentiation after implantation, the cells need to be labeled and imaged with high spatial resolution. For *in vivo* MRI detection at the cellular level, this has been achieved primarily with iron oxide nanoparticles, ultrasmall paramagnetic iron oxides (USPIOs), and SPIOs particles. These particles, which can be incorporated into the cells prior to transplantation, produce decreases in relaxivity time for T2*-weighted MRI or GRE imaging by virtue of susceptibility differences to the adjacent environment (Shapiro et al., 2004; Hoehn et al., 2007).

In previous studies, we used SPIOs to label adult human NSCs and tracked their migration in host human brains following transplantation (Zhu et al., 2006). In this study, we labeled iPSCs-derived NSCs with SPIOs and then imaged labeled cell distribution in host animal brains and spinal cords *in vivo*. We detected hypointense signals in animals that received SPIO-labeled NSCs treatment at the cell injection site and around the injury region (Fig. 3). PB staining of brain sections revealed migrated NSCs within and around the lesion. No hypointense signal change was observed in animals that did not receive NSCs implantation or that received PBS therapy. Concomitant with transplanted cell migration, animals in experimental groups showed improved motor function relative to the control group animals (Fig. 3 and video). Moreover, the immunohistochemistry of rat brain sections showed that the implanted NSCs can differentiate into functional neural cells and participate in the local neural circuit (Fig. 3H).

In this study, we have demonstrated for the first time, to the best of our knowledge, the possibility of *in vivo* iPSCs-derived NSCs tracking. Additionally, MRI tracking of labeled cells from the area of cell injection sites to lesion regions in small and large animal CNS injury models provides evidence for the safety of this imaging technique. These data pave the way for future research protocols for noninvasive tracking of iPSCs-derived NSCs.

Despite the interesting results of the study, some problems must be resolved before iPSCs and their derivates could be applied for clinical patients (Wernig et al., 2008). The safety of iPSCs transplantation is a serious concern. In our experiment, none of the animals developed tumors (Fig. 3). However, the results from our study were a short-term conclusion. Furthermore, long-period studies should be conducted to test the safety of iPSCs transplantation before this technique can be applied to a clinical context.

In conclusion, this study demonstrated the survival and targeted migration of iPSCs-derived NSCs *in vivo* for the first time in the literature. Furthermore, the motor function improvement of injured rats and monkeys after iPSCs replacement therapy suggested functional integration of the transplantation cells into the lesion tissue from *in vivo* levels. Our results indicated the clinical viability and potential of iPSCs derivatives for CNS injury therapy.

Acknowledgments

We are grateful to the technicians (Luping Chen, Yiwen Shen, and Qisheng Tang) in the stem cell lab for their assistance in animal preparation and advice on experiments. This work was supported by grants (81200936, 2010CB945500, 2012CB966300, 11JC1401000, 2009CB941100) from National Nature Science Foundation, Ministry of Science and Technology of China and Shanghai City Science Foundation, and 2011 Shanghai Medical College Young Scientist Fund of Fudan University (11L-24).

Author Disclosure Statement

The authors declare that no conflicting financial interests exist.

References

Allen, A.R., and Mac Phail, R.C. (1991). Surgery of experimental lesion of spinal cord equivalent to crush injury of fractured is location of spinal column. Pharmacol. Biochem. Behav. 57, 878–880.

Breunig, J.J., Haydar, T.F., and Rakic, P. (2011). Neural stem cells: Historical perspective and future prospects. Neuron 70, 614–625.

Chambers, S.M., Fasano, C.A., Papapetrou, E.P., et al. (2009). Highly efficient neural conversion of human ES and iPS cells by dual inhibition of SMAD signaling. Nature Biotechnol. 27, 275–280.

Dixon, E., Clifton, G., and Lighthall, J.W. (1991). A controlled cortical impact model of traumatic brain injury in rat. J. Neurosci. Methods 39, 253–262.

Feeney, D.M., Boyeson, M.G., Linn, R.T., et al. (1981). Response to cortical injury: 1 methodology and local effects of contusions in the rat. Brain Res. 211, 67–77.

Henrich, C., Cao, Y.H., and Lars, O. (1996). Spinal cord repair in adult paraplegic rats: Partial restoration of hind limb function. Science 273, 510–513.

Hoehn, M., Wiedermann, D., Justicia, C, et al. (2007). Cell tracking using magnetic resonance imaging. J. Physiol. 584, 25–30.

Jaenisch, R., and Young, R. (2008). Stem cells, the molecular circuitry of pluripotency and nuclear reprogramming. Cell 132, 567–582.

Mahmood, A., Lu, D., Wang, L., et al. (2001). Treatment of traumatic brain injury in female rats with intravenous administration of bone marrow stromal cells. Neurosurgery 49, 1196–1203.

Neri, M., Maderna, C., Cavazzin, C., et al. (2008). Efficient in vitro labeling of human neural precursor cells with superparamagnetic iron oxide particles: Relevance for in vivo cell tracking. Stem Cells 26, 505–516.

Postmantur, R., Kampel, A., and Simon, R. (1997). A calpain inhibitor attenuates cortical cytoskeletal protein loss after experimental traumatic brain injury in the rat. Neuroscience 77, 765–787.

Robinton, D.A., and Daley, G.Q. (2012). The promise of induced pluripotent stem cells in research and therapy. Nature 481, 295–305.

Shapiro, E.M., Gonzalez-Perez, O., Manuel García-Verdugo, J., et al. (2006). Magnetic resonance imaging of the migration of neuronal precursors generated in the adult rodent brain. Neuroimage 32, 1150–1157.

Shapiro, E.M., Skrtic, S., Sharer, K., et al. (2004). MRI detection of single particles for cellular imaging. Proc. Natl. Acad. Sci. USA 101, 10901–10916.

Takahashi, K., and Yamanaka, S. (2006). Induction of pluripotent stem cells from mouse embryonic and adult fibroblast cultures by defined factors. Cell 126, 663–676.

Takahashi, K., Okita, K., Nakagawa, M., et al. (2007a). Induction of pluripotent stem cells from fibroblast cultures. Nat. Protoc. 2, 3081–3089.

Takahashi, K., Tanabe, K., Ohnuki, M., et al. (2007b). Induction of pluripotent stem cells from adult human fibroblasts by defined factors. Cell 131, 861–872.

Villegas, J., and McPhaul, M. (2005). Establishment and culture of human skin fibroblasts. Curr. Protoc. Mol. Biol., Chapter 28: Unit 28.3. doi: 10.1002/0471142727.mb2803s71.

Wernig, M., Meissner, A., Cassady, J., et al. (2008). c-Myc is dispensable for direct reprogramming of mouse fibroblasts. Cell Stem Cell 2, 10–12.

Zhu, J., Zhou, L., Xing, W., et al. (2006). Tracking neural stem cells in patients with brain trauma. N. Engl. J. Med. 355, 2376–2378.

Address correspondence to:
Dr. Xiaoyuan Feng
Radiology Department
HuaShan Hospital
Shanghai, China

E-mail: xyfeng@fudan.edu.cn

and

Jianhong Zhu
Neurosurgery Department
HuaShan Hospital
No. 12, Middle Wulumuqi Road
Shanghai 200040, China

E-mail: jzhu@fudan.edu.cn